1710. Effects of brake pressures on stick-slip bifurcation and chaos of the vehicle brake system

Daogao Wei[1], Weiwei Zhu[2], Bo Wang[3], Qian Ma[4], Zuheng Kang[5]
[1, 2, 3]School of Mechanical and Automotive Engineering, Hefei University of Technology, Hefei, 23009, China
[4]Jiangsu Xuzhou Construction Machinery Institute XCMG, Xuzhou, 221004, China
[5]Mechanical and Aerospace Engineering, University of Missouri, Columbia, MO, 65201, USA
[1]Corresponding author
E-mail: [1]*weidaogao@hfut.edu.cn*, [2]*david2009138020@163.com*, [3]*wangbo.lucky@163.com*, [4]*maqian5516@126.com*, [5]*zkbrc@mail.missouri.edu*

(Received 16 December 2014; received in revised form 9 February 2015; accepted 10 April 2015)

Abstract. Vibrations and noises induced by vehicle braking at low speeds are problems that have always blocked the development of the automotive industry, which the stick-slip vibrations of brake system are the major reason that causes the vibration and noise. Ref. [19] predicts chaotic stick-slip vibrations by introducing a torsional model. Additionally, in this article, we have established a four degree of freedom torsional braking model under pure braking, which is based on that reference. Since the chaotic stick-slip motions have been found based on a proper friction model through numerical method, from the bifurcation diagram of the relative velocity between the rotor and pad to corresponding brake pressure, we also found the dynamic characteristics of the system changing from doubling periodic bifurcation to chaos just by increasing the brake pressures. Any further numerical study showed that the doubling periodic bifurcation occurs both in stick phase and slip phase, which composed of the upper and lower bifurcation of the global bifurcation diagram. Thus, chaos and periodic motions in it can be identified by calculating Lyapunov exponents with 'CLDYN' method. At last, the effects of friction model parameters on bifurcation and chaos were studied, which provides important evidence theoretically showing that the decrease in braking vibrations and noises at low speed and the matching control of braking pressures.

Keywords: friction pair, stick-slip, doubling periodic bifurcation, chaos, Lyapunov exponent.

1. Introduction

Because of the problem of brake vibrations and noises of automobiles at low speeds is still unresolved, and its mechanism is also not entirely clear for us [1-4], however, it is generally believed that the stick-slip vibrations is the main reason of the brake vibrations at low speeds, and bifurcation and chaos of vibrations are not negligible mechanisms that deteriorate vibrations and noises, therefore, many studies have been delivered by domestic and foreign scholars in this area. The current consensus is that the changes in the brake pressures lead to stick-slip friction excitations between the rotor and the pad at extremely low speeds, therefore generates a series of phenomenon called low-speed brake squeal.

Early in 1938, Mills [5] had found that stick-slip vibration is one of the reasons that leads to the brake squeal when he was examining the drum brake squeal. Then he raised a concept of stick-slip, thinking that brake squeal was associated with the decrease in friction coefficient with rubbing speed. His work led to a school of scholars beginning to study on stick-slip vibrations. In fact, Bowden [6] and Morgan's [7] works on stick-slip vibrations in friction oscillators confirmed Mills' experiment results. Both of them share an idea that the necessary condition for a brake to vibrate is the negative correlations between friction and velocity. In order to explore the mechanism of stick-slip vibrations, many scholars conducted researches deeply with a simple one degree of freedom of slider – sliding belt model. Meantime, F. Van De Velde and P. De Baets [8] also find this phenomenon through their experiment, but additionally find the hysteretic effects between friction and velocity. U. Andreaus and P. Casin [9] further studied the effects of the belt

speed on system's stick-slip vibrations, and found a critical value of the belt speed, which is the speed of higher bound of stick-slip vibrations. Yong Li [10] applied the dry friction model in Ref. [11] and found there exist a stable limit cycle and chaotic motions of the dynamic system based on previous slider-belt model, and she also found that stick-slip motion would occur at a relatively low speed. Oestreich [12] studied the effects of the frequency of harmonic external excitation on bifurcation and chaos of the slider-belt system, and found the system has complicated dynamic characteristics of period doubling bifurcation to chaos through the changing of the external excitation frequencies. Peter [13] studied the stick-slip motions of two-mass mechanical system with a driven force in different friction conditions, and found the stick-slip motions mainly depend on the properties of the mechanical system, especially on the drive, and rather on different characteristics of the friction model.

Several researches above of the mechanism and the phenomenon of stick-slip showing that different scholars built different stick-slip vibration model of brake system, and these models can be generally classified into two categories: one is the tangential vibration model, and the other is the torsional vibration model. The first one is directly evolved from the slider-belt model, which has been comparatively studied and developed – K. Shin [14, 15] simplified the rotor and pad into a one degree of freedom system respectively, and coupled through a friction pair. Based on this model, he studied the effects of system's damping on stick-slip motions, and found that the damping of the rotor and the pad are also fundamental to the stability of the system. Manish Paliwal [16] believe the interfacial coupling stiffness between the rotor and the pad will change while braking, and the effects on stick-slip motions can never be neglected. Then he added a coupling stiffness between the rotor and pad on K. Shin's model, and studied the influences of coupling stiffness on the stability and the stick-slip motions of the system. Yang [17] studied the period doubling bifurcation and chaos of the brake system with the change of disc speeds, and analyzed the influences of damping on the bifurcation and chaos. Different from the above scholars' tangential vibration model, Li Bo and Ding Qian [18] comprehensively considered the tangential and torsional vibrations of the pad, and learned the influences of disc speeds and the viscous friction factor of the LuGre friction model on the tangential and torsional stick-slip vibrations. In sum, their work showed that with the decrease of the disc velocity, and the tangential motions of the pad lose its stability, the stick-slip vibrations will occur, and the chaotic stick-slip motions can be resulted as the viscous factor becoming large.

The tangential vibration model seemingly has many advantages and it is convenient for research because of its simple structure, which the influences of other sub-systems of the whole vehicle system on the brake system could be approximately ignored. However, since the motions of automobile's driving and braking belong to rotary motions, its torsional vibration can never be neglected. Crowther [19, 20], in order to avoid this deficiency, firstly proposed a four degree of freedom torsional model, including driveline and brake torsional sub-systems coupled through a friction pair by studying the stick-slip motions of the coupled system under low constant drive torque according to Coulomb's law, and found three types of stick-slip motions with different brake pressures. He also predicted the motion of the system might contain chaotic characteristics, but eventually failed to prove it. Jin Zhang [21] simplifies his four degrees of freedom torsional model into a two degree of freedom model by studying the periodic stick-slip motions of the system under different driving speeds, and then find that the higher the driving speeds is, the longer and higher the slip phase and the stick-slip frequency would be.

In sum, many researchers and scholars have seen many phenomena related to the chaotic stick-slip vibrations of the brake system under different friction models through tangential vibration model. However, none of those ever did researches about chaotic vibrations through torsional vibration model; thus the effects of brake pressures on system's vibrations that are limited to periodic vibrations, and researches about the effects of brake pressures on chaotic vibrations are never been found. Thus, in this article, we establish a four degree of freedom torsional vibration model under pure braking condition based on the coupled system proposed in Ref. [19] by using a light truck as prototypes, and studied the influences of brake pressures on

bifurcation and chaos of the system with phase planes and Lyapunov exponent by numerical method and find another several important mechanisms of torsional and chaotic stick-slip motions under low speeds. Also, we hope to provide theoretical references to reduce the vibration and noise of this type.

2. Build a dynamic model for vehicle brake system

2.1. Dynamic model and equations of motion for vehicle brake system

In this article, we establish a four degree of freedom torsional model under pure braking condition based on the driven model mentioned in ref. [19]. Its mechanical model is shown in Fig. 1, including driveline and brake torsional sub-systems, with friction interface through the rotor and the pad. The brake sub-system (shown in Fig. 1(b)) which would include brake caliper, knuckle and suspension components is simplified to a disc, and its moment of inertia is denoted as J_4. The driveline dynamics (shown in Fig. 1(a)) can be divided into three inertias: J_1 representing the equivalent inertia of the final drive and half axle; J_2 is the equivalent inertia of the brake rotor, wheel hubs and rims; J_3 is the equivalent inertia of the tire and the vehicle mass. These inertias are connected via two torsional stiffness elements: k_1, an equivalent stiffness of half axle; k_2, the tire stiffness. k_3 is the equivalent stiffness of brake. The terms c_1, c_2, c_3 is the viscous damping along with stiffness elements, and d_1 is the equivalent damping counting the friction of the components of the final drive and the differential. Fig.1c is the side view of brake disc and tire. r_b is the average radius of contact between the brake pad and brake disc, R is the radius of wheel rolling, V is the vehicle speed, F_b is the brake friction force, F_μ is the ground brake force. θ_y is the rotating angle of the system. T_r, T_t, T_b are the torques that act on the brake disc, the tire and the brake pad. Two assumptions are made to build this mechanical model: 1) the mass center of equivalent disc lies on the rim, 2) wheels can only consider to be pure rolling when calculating vehicle speeds in the process of braking.

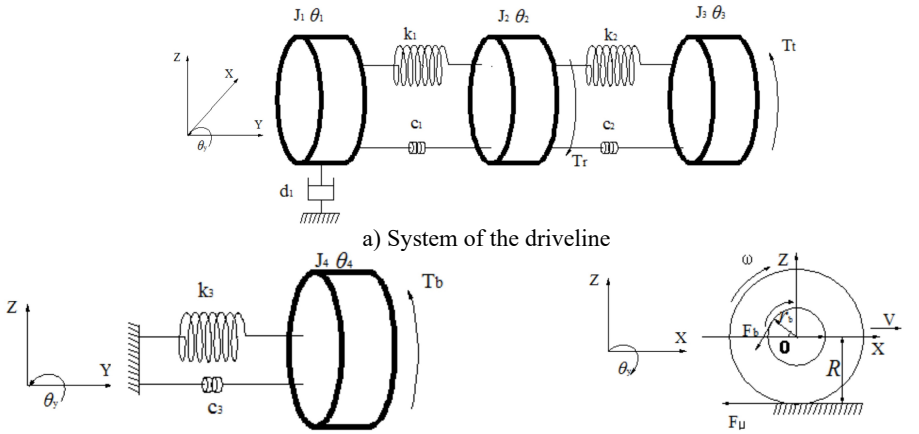

a) System of the driveline

b) Brake sub-system

c) Rotor/tire side view

Fig. 1. 4-DOF brake torsional model

Based on the dynamic model shown in Fig. 1, the differential equation of the 4-DOF system rotating along the Y-axle can be derived by using Lagrange's equation:

$$\frac{d}{dt}\left(\frac{\partial E_T}{\partial \dot{\theta}_i}\right) - \frac{\partial E_T}{\partial \theta_i} + \frac{\partial E_V}{\partial \theta_i} + \frac{\partial E_D}{\partial \dot{\theta}_i} = Q_i, \tag{1}$$

where θ_i is generalized coordinates; E_T is total kinetic energy; E_V is total potential energy; E_D is

total dissipative function; Q_i is generalized forces. In this system, E_T, E_V, E_D and Q_i can be expressed as:

$$\begin{cases} E_T = \frac{1}{2}J_1\dot{\theta}_1^2 + \frac{1}{2}J_2\dot{\theta}_2^2 + \frac{1}{2}J_3\dot{\theta}_3^2 + \frac{1}{2}J_4\dot{\theta}_4^2, \\ E_D = \frac{1}{2}d_1\dot{\theta}_1^2 + \frac{1}{2}c_1\left(\dot{\theta}_1 - \dot{\theta}_2\right)^2 + \frac{1}{2}c_2\left(\dot{\theta}_2 - \dot{\theta}_3\right)^2 + \frac{1}{2}c_3\dot{\theta}_4^2, \\ E_V = \frac{1}{2}k_1(\theta_1 - \theta_2)^2 + \frac{1}{2}k_2(\theta_2 - \theta_3)^2 + \frac{1}{2}k_3\theta_4^2, \\ Q_i = T_{r/b}\frac{\partial\left(\dot{\theta}_2 - \dot{\theta}_4\right)}{\partial\theta_i} + T_t\frac{\partial\dot{\theta}_3}{\partial\theta_i}. \end{cases} \tag{2}$$

Substituting Eq. (2) into Eq. (1), then could obtains the differential equation of the system:

$$\begin{cases} J_1\ddot{\theta}_1 + d_1\dot{\theta}_1 + c_1\left(\dot{\theta}_1 - \dot{\theta}_2\right) + k_1(\theta_1 - \theta_2) = 0, \\ J_2\ddot{\theta}_2 + c_1\left(\dot{\theta}_2 - \dot{\theta}_1\right) + c_2\left(\dot{\theta}_2 - \dot{\theta}_3\right) + k_1(\theta_2 - \theta_1) + k_2(\theta_2 - \theta_3) = T_r, \\ J_3\ddot{\theta}_3 + c_2\left(\dot{\theta}_3 - \dot{\theta}_2\right) + k_2(\theta_3 - \theta_2) = T_t, \\ J_4\ddot{\theta}_4 + c_3\dot{\theta}_4 + k_3\theta_4 = T_b. \end{cases} \tag{3}$$

2.2. Selection of dry friction model

Due to the complexity of the behavior of the system vary from friction parameter, a unified model cannot be established to illustrate the different dynamic characteristics of mechanics. Different scholars proposed different friction models to study particular dynamic characteristics of mechanical systems [22]. Generally, it's believed that the decrease in friction coefficient with rubbing speeds is the reason that leads to stick-slip motions of the system, though different friction models may lead to different types of stick-slip motions. Thus, this paper selects the dry friction model shown in Ref. [23], which is smoothed with a factor σ by a hyper-tangent function. The relations between friction coefficient and relative velocity can be denoted as:

$$\mu\left(\dot{\delta}_0\right) = \mu_k\left[1.0 + \left(\frac{1}{\xi} - 1.0\right)e^{-\alpha|\dot{\delta}_0|}\right]\tanh\left(\sigma\dot{\delta}_0\right), \tag{4}$$

where α defines exponential decay factor, $\alpha = 2$; σ defines the smooth factor ($\sigma = 50$); ξ defines the ratio of the kinetic friction coefficient μ_k and the static friction coefficient μ_s, namely, $\xi = \mu_k/\mu_s$. According to the measurement of the kinetic and static friction coefficient about several friction materials of brake friction pairs in Ref. [24], in this paper, we select $\mu_s = 0.6$ and $\mu_k = 0.65\mu s$.

In order to explore the vehicle's dynamic characteristics at a particular constant speed rather than the whole braking process, a constant excitation of forward speed V is assumed to be given to the system. Since the automobile has been in a state of pure rolling, the functional relationships of wheel rotate speeds and the forward speeds of the vehicle can be approximately expressed as:

$$\omega = \frac{V}{R}, \tag{5}$$

where ω defines the wheel rotation speed, V defines the forward speed of the vehicle.

$\dot{\delta}_0$ is the relative angular velocity between rotor and brake in the friction model of Eq. (4). The driveline system gets a constant excitation of angular velocity ω which can be transformed from the vehicle speed. So $\dot{\delta}_0$ can be denoted as:

$$\dot{\delta}_0 = \omega + \dot{\theta}_2 - \dot{\theta}_4. \tag{6}$$

Then the friction torque is:

$$T_b = -T_r = F_b \cdot r_b = F_N \cdot \mu(\dot{\delta}_0) \cdot r_b, \tag{7}$$

where F_N defines brake pressure between brake disc and brake pad.

Considering the complexity of the dynamic behavior of friction between the wheel and the ground, it can be denoted neither by bringing forth the existed friction model of tire, nor equaling it to a damping similar to Ref. [19]. According to the analysis of the statics, the torque acting on the tire from the ground is approximately equivalent to the brake torque acting on the disc at slow speed. Then, it can be expressed as:

$$T_t = F_\mu \cdot R = \frac{F_\mathrm{b} \cdot r_b}{R} \cdot R = F_\mathrm{b} \cdot r_b = T_b. \tag{8}$$

Fig. 2 illustrates μ as a function of relative angular velocity $\dot{\delta}_0$ and the effects of smoothening on it, which are calculated by numerical methods based on the chosen friction model. The friction coefficient shows strong nonlinear and negative slope characteristics when the relative velocity is low as shown in Fig. 2, then tends to fix value at a high relative velocity.

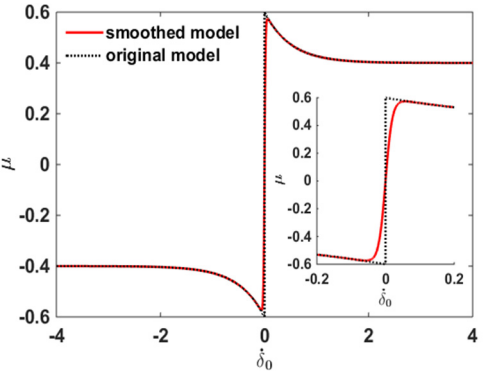

Fig. 2. The friction coefficient as a function of relative angular velocity and zoomed part

3. Analyses of bifurcation and chaos properties

In order to analyze the chaotic properties, in this article, we are based on a group of parameters obtained from a sample car (shown in Table 1). Then, establishing differential equations based on the dynamic model of braking system, and the friction model; the bifurcation characteristics of stick-slip motions related to brake pressures can be calculated by Runge-Kutta 4, 5 method with adaptive step size control.

Table 1. Calculating parameters

Parameter	J_1 / kg·m^2	J_2 / kg·m^2	J_3 / kg·m^2	J_4 / kg·m^2	k_1 / N·m·rad
Value	0.0018	0.1094	6.2500	0.0625	5.31×10^4
Parameter	k_2 / N·m·rad	k_3 / N·m·rad	c_1 / N·m·rad/s	c_2 / N·m·rad/s	c_3 / N·m·rad/s
Value	1.41×10^6	2×10^5	1	3	20
Parameter	d_1 / N·m·rad/s	F_N / N·m	R / m	r_b / m	
Value	30	1000	0.35	0.13	

There is a common view about the mechanism of stick-slip vibrations that there exist a boundary value of relative velocity δ_0. The stick-slip motions will usually occur when $\delta < \delta_0$,

and disappear at $\delta > \delta_0$. To control the relative velocity δ between the rotor and pad bellow the critical velocity δ_0, the lower vehicle speed ($V = 0.05$ m/s) was selected.

Employing the brake pressure F_N as one of a bifurcation parameter, then the system global bifurcation characteristics $\dot{\delta} - F_N$ can be calculated (shown in Fig. 3) based on system dynamic Eqs. (3)-(8) (parameters shown in Table 1).

From Fig. 3, when the brake pressures are between 300 N and 2000 N, with the increase of the brake pressures, the stick-slip vibration characteristics of the system will change from double periodic bifurcation to chaos under the selected vehicle speed. The content of this paper is arranged as follows: firstly, analyzed the effects of brake pressures on stick-slip vibration characteristics of the system through selecting the values of brake pressures corresponding to the typical bifurcation and chaos, then calculated Lyapunov exponent of the system to distinguish between chaos and periodic motions. Finally, the effects of friction model parameters on bifurcation and chaos were studied.

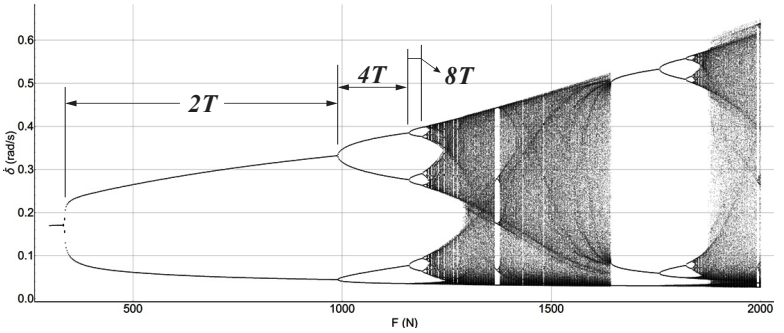

Fig. 3. Bifurcation diagram employing F_N as a bifurcation parameter

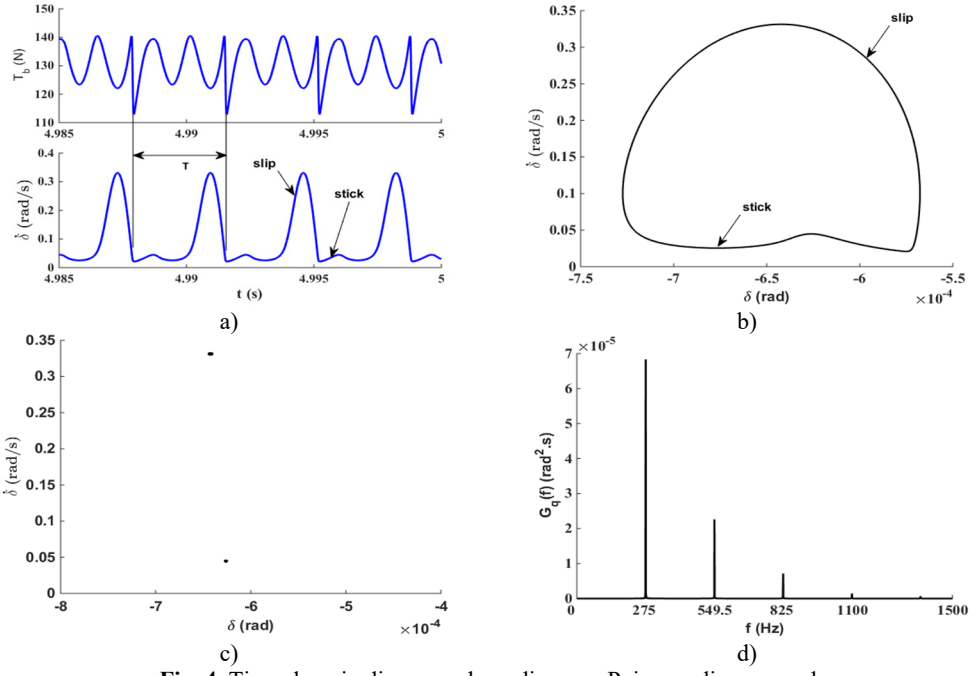

Fig. 4. Time-domain diagram, phase diagram, Poincare diagram and power spectrum diagram under $F_N = 980$ N

Arbitrarily selecting values of brake pressure in the periodic region of $2T$, $4T$, $8T$ and chaotic

region respectively according to Fig. 3, and calculating the vibration characteristics of the relative velocity between the rotor and the pad. For example, we can select F_N = 980 N, 1100 N, 1180 N, 1320 N respectively, and then get the Time-Domain Diagram, Phase Diagram, Poincare Map and Power Spectrum under these F_N through numerical calculations (shown in Figs. 4-7).

The system's motions are not strictly a stick-slip vibration from the time-domain diagram of friction torque and the relative velocities shown in Fig. 4(a). In the stick phase, the value of the relative velocity between the rotor and the pad is not always zero, however, the fluctuation around a value will be slightly larger above zero, which causes the bottom of the limit cycle will not be a straight line, but a tiny hump (shown in Fig. 4(b)). In the slip phase, the friction torque will not be a constant value but with a larger fluctuation due to the friction model we selected differs from the Coulomb's law. The value of kinetic coefficient will be a constant value when the relative velocity is nonzero under the Coulomb's law, so the friction torque remains unchanged, shown in Ref. [19]. Since the friction model selected in this paper has an obvious negative slop of the kinetic coefficient under a lower relative velocity, the friction torque will fluctuate in the slip phase; the values of friction torque suddenly drop while the motions of the system changing from slip to stick by comparing with the time-domain diagram of friction torque and relative velocity, shown in Fig. 4(a). This figure also shows that the system has two period stick-slip motions in the Poincare diagram (Fig. 4(c)) and power spectrum (Fig. 4(d)); the fundamental frequency is 549.5 Hz, the fractional frequency is 275 Hz, and the peak value of the latter is 3.02 times larger than the former.

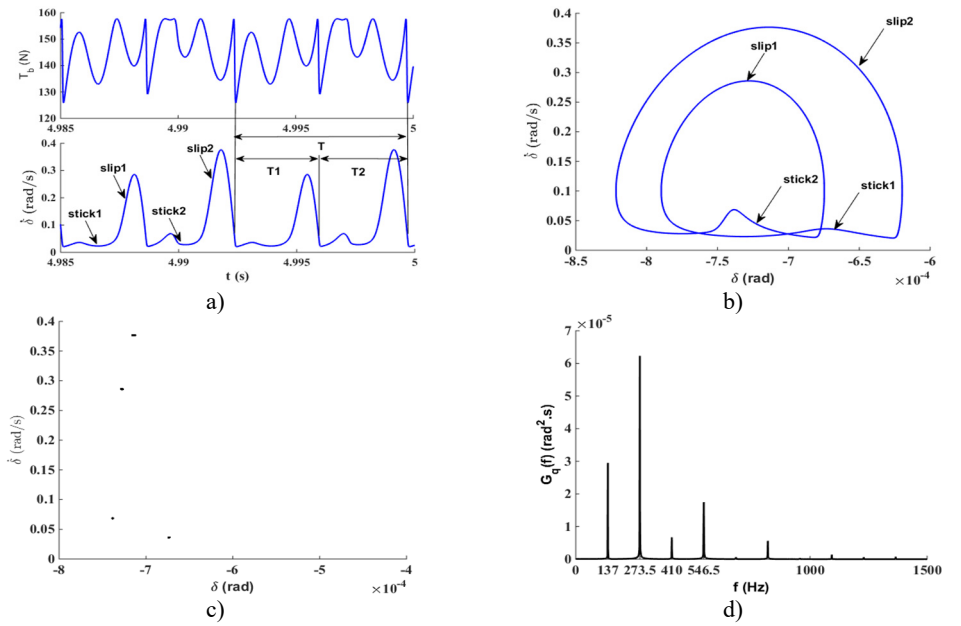

Fig. 5. Time-domain diagram, phase diagram, Poincare diagram and power spectrum diagram under F_N = 1100 N

Fig. 5 shows that the system has four period stick-slip motions. In period T, there exist two types of stick-slip vibrations –T_1 and T_2, shown in Fig. 5(a) and Fig. 5(b). In the second stick phase (stick 2), the fluctuation of relative velocities is larger than the first stick phase (stick 1), which corresponds to the lower branch of the global bifurcation diagram. However, the peak value of the relative velocities in the first slip phase (slip 1) is smaller than that in the second slip phase (slip 2), which corresponds to the upper branch of the global bifurcation diagram. We can also see that the system has four period stick-slip motions in the Poincare diagram (Fig. 5(c)) and power spectrum (Fig. 5(d)), and its fundamental frequency is 546.5 Hz. Additionally, the system also has the 1/4 fractional frequency of 137 Hz, the 1/2 fractional frequency of 273.5 and the 3/4 fractional

frequency of 410 Hz, and the peak value of the 1/2 fractional frequency is the maximum, which is 3.57 times larger than the fundamental frequency.

Fig. 6 illustrates that the system has an eight-period stick-slip motions under the brake pressure $F_N = 1180$ N. In period T, there exist four types of stick-slip vibrations shown in Fig. 6(a) and Fig. 6(b). Among these four types of stick-slip periods, the high fluctuation and a low fluctuation of the relative velocities will appear periodically both in the stick phase and the slip phase, which forms the eight-period motions of the system. But compared with the double-period motions (Fig. 4) and the four-period motions (Fig. 5), the fluctuation of relative velocities will become bigger and bigger in the stick phase, which leads to the bifurcation mainly growing towards the upper bifurcation, while the shape of lower bifurcation becomes more straight, which makes the global bifurcation diagram (Fig. 3) appears to be a squashed doubling periodic bifurcation. Fig. 6 also shows that the system has eight-period stick-slip motions in the Poincare diagram (Fig. 6(c)) and power spectrum (Fig. 6(d)). Its fundamental frequency is 545 Hz accompanied with some other harmonic frequencies.

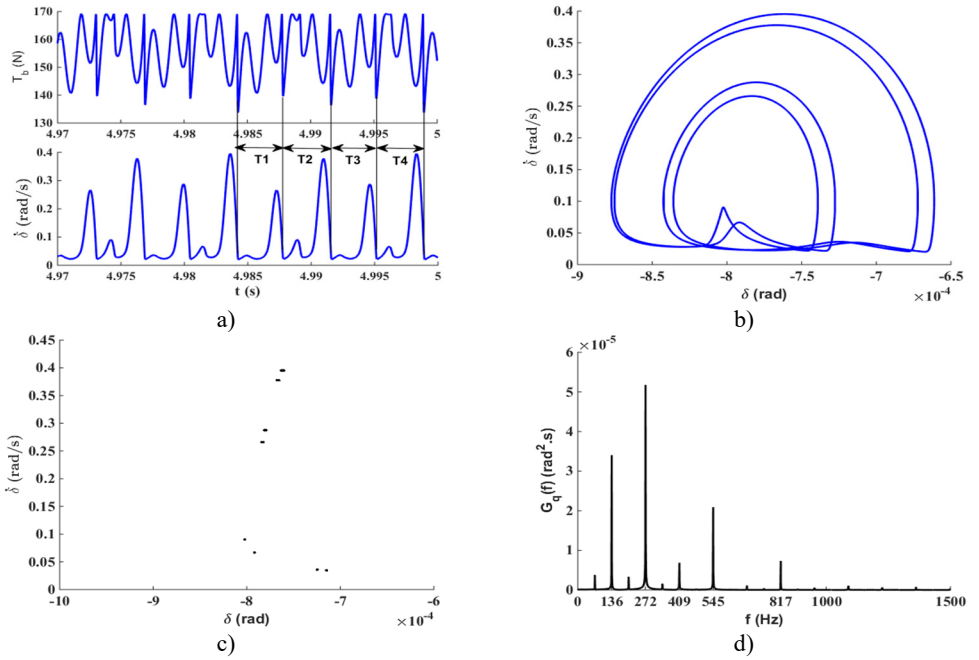

Fig. 6. Time-domain diagram, phase diagram, Poincare diagram and power spectrum diagram under $F_N = 1180$ N

The motions of the system will turn into chaotic vibrations under the brake pressure $F_N = 1320$ N, as shown in Fig. 7. The attractor of the system has obvious self-similarity properties shown in the Poincare diagram (Fig. 7(d)) and the power spectrum of relative velocities (Fig. 7(e)) shows a background which is similar to that of noises. Fig. 7(a), (b) shows the time-domain diagram of the friction torque and relative velocities after adding a small perturbation Δ ($\Delta = 0.001$ rad) to the initial angular velocity of the rotor, which indicates that the friction torque and relative velocities have a highly sensitivity at the initial condition. In the test, the trajectory of perturbation is similar to the first one in the time before 0.08 second, but the difference between these two trajectories will become larger with a tiny perturbation as the time goes. When $t = 0.1656$ s, the value of friction torque on original trajectory is 188.4 N/m, while the corresponding value on the perturbation trajectory is 146.5 N/m, and the former is 0.28 times larger than the latter. Similarly, the value of relative velocity on original trajectory is 8.24 times larger than that on perturbation trajectory when $t = 0.1888$ s.

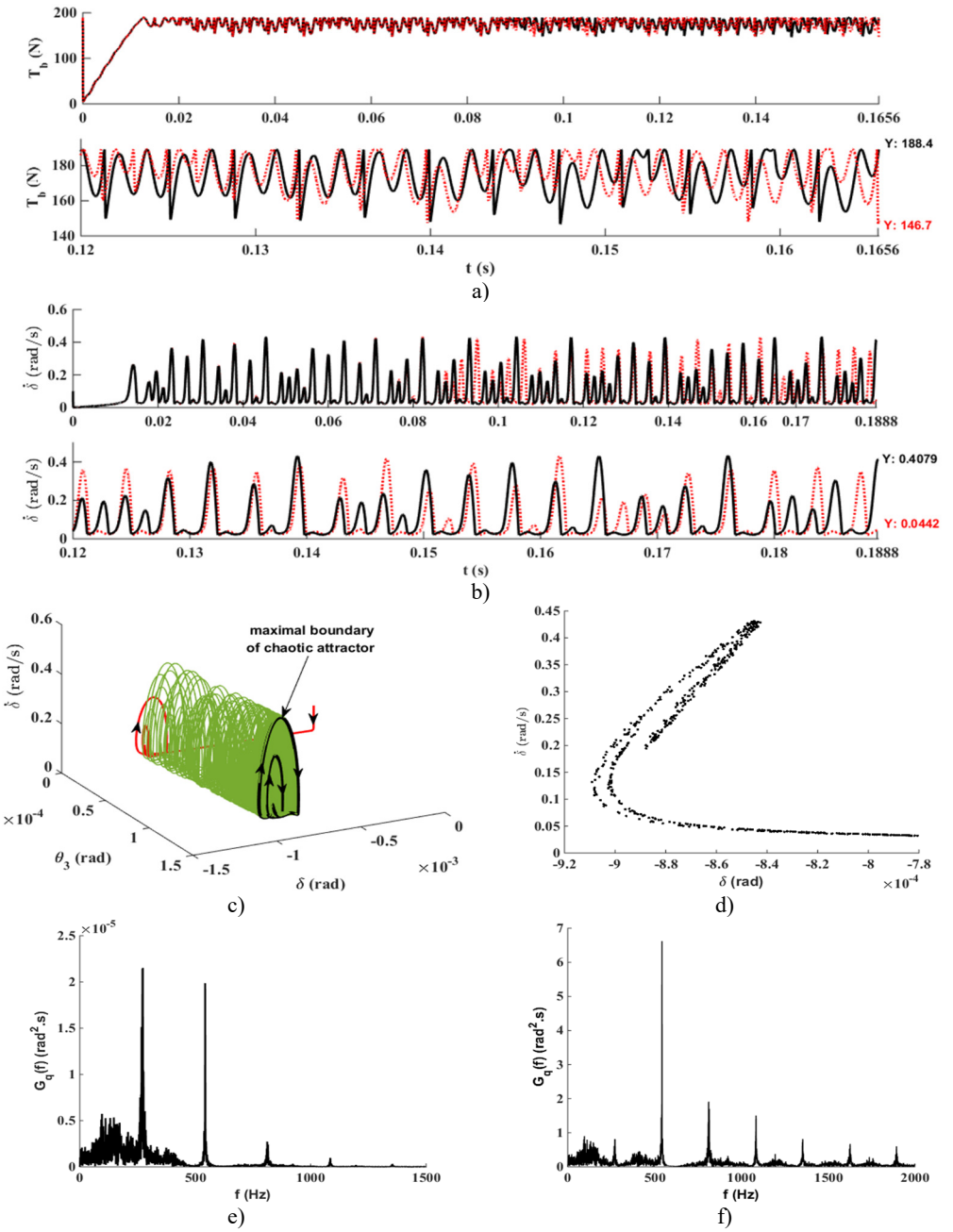

Fig. 7. Time-domain diagram, phase diagram, Poincare diagram and power spectrum diagram under $F_N = 1320$ N

In Fig. 7(b),(c), the fluctuation of relative velocity so large that it cannot be regarded as a fluctuation in the stick phase, but a slip motion; then the occurrences of 'stick' and 'slip' appears to be irregular and random, and hence the stick-slip motions turn into chaos. Fig. 7(f) shows the spectrum diagram of the friction torque; the frequency spectrum is obviously continuous, which indicates that the motions of friction torque are in the chaotic state. The chaotic motions of the friction torque with the vibrations and noises deteriorate the stability under driving conditions such as the release of the brake on takeoff and the brake of the vehicle to stop.

4. Identification of periodic solution and chaos by Lyapunov exponent

It is easy to identify the type of motions, whether it is period or chaos under a specific bifurcation parameter through Poincare diagram and spectrum diagram from the analysis above. However, it's arduous and unrealistic to identify the type of motions for each parameter of this method, especially for the range of bifurcation parameter becomes really large in $\dot{\delta} - F_N$ bifurcation diagram, shown in Fig. 3. To avoid this deficiency and to obtain the interval of period and chaos, identifying the type of the system's motions through calculating the Lyapunov exponent, which is an important quantitative index to measure the dynamic characteristics of the system and to character the average index ratio of convergence or divergence between two adjacent trajectories in the phase space, may be a good approach. This method can clearly identify periodic solutions and chaos of the system, particularly for the periodic solutions within the interval of chaos.

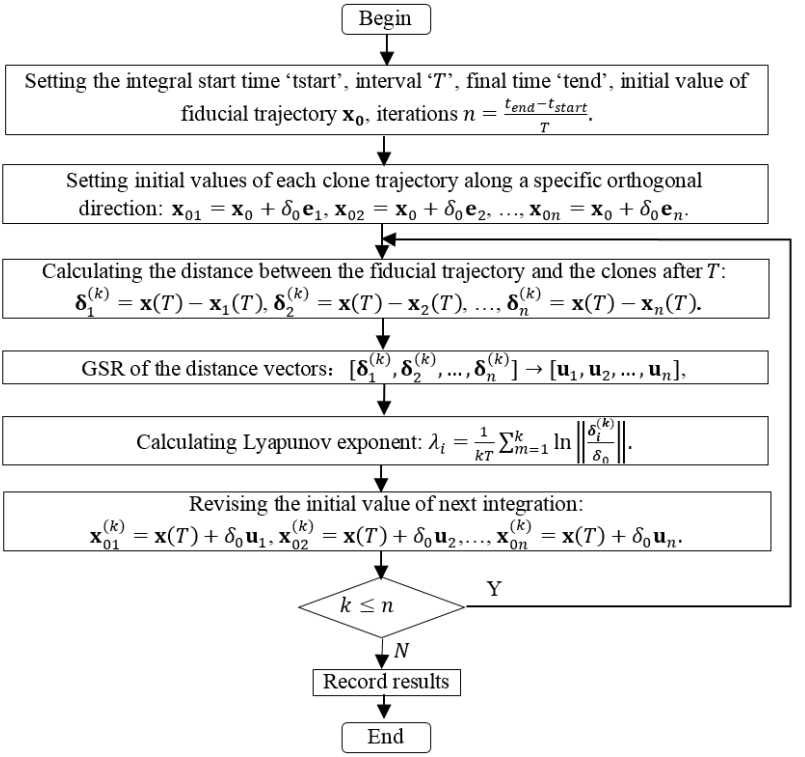

Fig. 8. The flow chart of calculating Lyapunov exponent

In this article, the 'CLDYN' method proposed in Ref. [25] was applied to calculate the Lyapunov exponent spectrum. This method analyzes the evolution of the difference state vectors defined as the distance between the fiducial trajectory and the clones of these motion equations initially being disturbed by small values in orthogonal directions. The complete Lyapunov exponent spectrum can be obtained by adding a small perturbation on each orthogonal direction. Since the system changes its orientation continuously, it is impossible to define a specific axis of the phase space as either expansive or contractive. Moreover, the orthogonal directions tend to align in the most expansive direction as the dynamical system evolves, which leads to the failure of the calculation of Lyapunov exponent. Thus, another method – the Gram-Schmidt Reorthonormalization (GSR) – was used to calibrate the orthogonal directions. A flow chart (Fig. 8) shows the calculation of the Lyapunov exponent.

Selecting $\delta_0 = 10^{-5}$, $T = 0.01$, and iterations $n = 10^4$, then, we can obtain the Lyapunov exponent spectrum under a specific bifurcation parameter F_N according to the algorithm introduced by the flow chart. Since the largest value of Lyapunov exponent could sufficiently reflect the stability of the system, the maximum positive Lyapunov exponent represents chaos and the zero exponent represents the periodic motion, thus we only calculate the maximal Lyapunov exponent in this paper; in other words, only considering the maximum value from the entire exponent spectrum, and its direction will always towards the direction of maximal Lyapunov exponent. Fig. 9(b) shows the maximum Lyapunov exponent under the brake pressures at F_N = 1190-1500 N, which can be obtained by iteration of computation with the changing parameter F_N. Fig. 9(a) is one part of bifurcation diagram corresponding to the range of the brake pressures (1190-1500 N) from the global diagram (Fig. 3). In addition, the accuracy of the calculation could be improved by skipping the transient trajectory that the system has not arrived steady state.

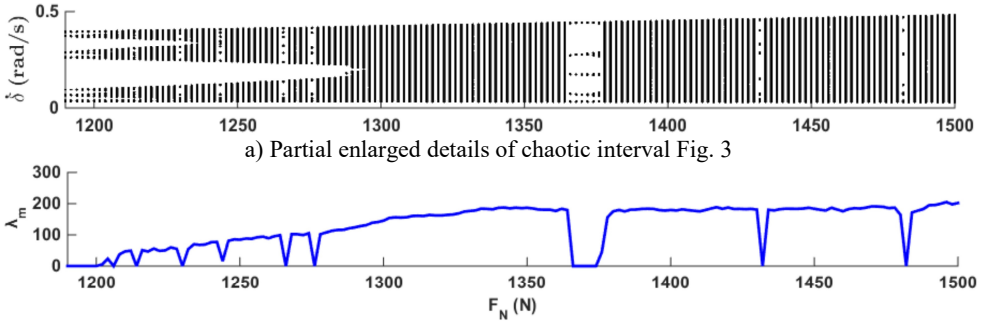

a) Partial enlarged details of chaotic interval Fig. 3

b) Maximal Lyapunov exponent corresponding to a)

Fig. 9. Partial bifurcation diagram and maximal Lyapunov exponent diagram

The maximum Lyapunov exponent could successfully distinguishes the periodic motions from the chaos. When the maximum Lyapunov exponent drops abruptly to zero, the motions will become the periodic motions, otherwise the chaos, as shown in Fig. 9(a), (b). Moreover, the maximum Lyapunov exponent becomes even larger after the merge of the upper branch and the lower branch at $F_N \approx$ 1300 N.

Table 2. Lyapunov exponent spectrum under F_N = 1200 N

λ_1	λ_2	λ_3	λ_4	λ_5	λ_6	λ_7	λ_8
0	–0.0410	–0.6081	–4.8002	–305.5453	–173.5329	–402.3243	–976.1830

Table 3. Lyapunov exponent spectrum under F_N = 1320 N

λ_1	λ_2	λ_3	λ_4	λ_5	λ_6	λ_7	λ_8
162.2937	1.0107	–0.0780	–4.7805	–291.3179	–31.6590	–318.2370	–821.2558

Table 4. Lyapunov exponent spectrum under F_N = 1370 N

λ_1	λ_2	λ_3	λ_4	λ_5	λ_6	λ_7	λ_8
0	–0.1585	–4.9395	–36.4785	–260.2797	–13.7716	–255.1294	–756.8736

Tables 2-4 shows the Lyapunov exponent spectrum when the brake pressures are selected to be three different values respectively, which is F_N = 1200 N, 1320 N, and 1370 N. When the maximal Lyapunov exponent is zero and the rest of Lyapunov exponent are negative (Tables 2, 4), it will be a periodic motion. However, when the maximal Lyapunov exponent to be positive, the motions of system will be chaos (Table 3).

5. Effects of friction model parameters on bifurcation and chaos

It is necessary to reduce chaotic vibrations of the brake system, since the mechanical with the property of wide-frequency performance and the complexity of the chaotic vibration could greatly declines the overall performance of mechanical systems, which may increase the vibrations and noises, the crack propagation, the fatigue and the friction of the material. The characteristics of friction pair is a crucial factor that induce stick-slip vibrations of brake system; the surface texture of friction pair could influence its friction characteristics because it causes the periodic fluctuation of friction coefficient. Appropriate surface texture would provide the approximately ideal friction characteristics which contains better performance of vibrations and noise of the brake system [26-29]. In order to find a proper friction parameters which might reduce the chaos, any researches on the effects of friction model parameter on bifurcation and chaos in brake system should be delivered, and the surface texture and ingredient design of friction pair would be the topic.

The Eq. (4) shows the friction model, where the exponential decay factor α and the ratio of the kinetic friction coefficient and the static friction coefficient ξ are the two key parameters which influence friction characteristics. The $\dot{\delta} - F_N$ bifurcation diagrams could be obtained from Eq. (3) by changing α and ξ respectively while remain other parameters kept unchanged as shown in Fig. 10. Fig. 10 (a) shows the bifurcation diagrams when ξ was selected to be 0.6, 0.65 and 0.7; we can see that the brake system has a similar dynamic behavior under different ξ, the dynamic behavior of the system will change from doubling periodic bifurcation to chaos along with the increase of the brake pressure, and periodic solution and chaos will appear alternately. But the intervals of brake pressure corresponding to a periodic solution expand as ξ increase in the studied pressure range. Fig. 10(b) is the bifurcation diagrams when select α to be 1, 2 and 3 respectively; we can see that the brake system has the similar dynamic behavior under different α, but the periodic interval will shrink and the chaotic interval will expand with α increases, thereafter the vibrations of brake system will be increased.

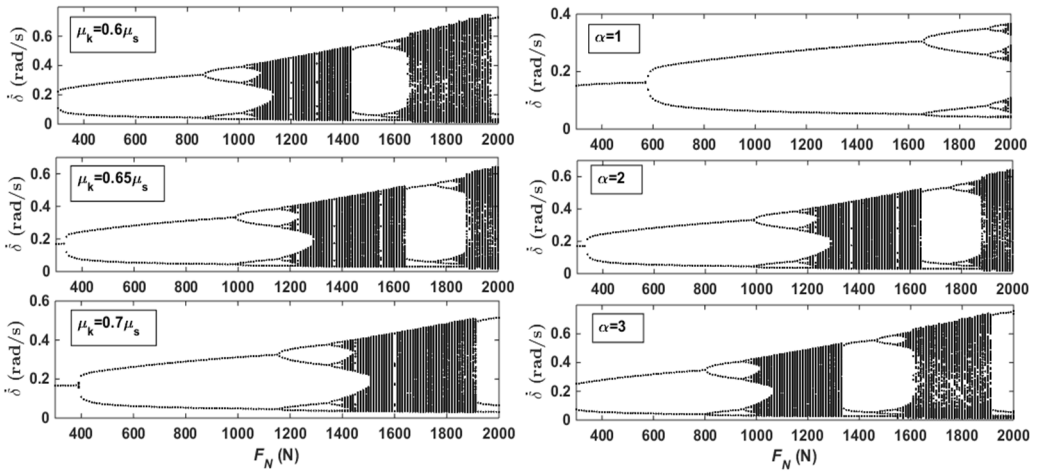

Fig. 10. The $\dot{\delta} - F_N$ bifurcation diagram of brake system under different α and ξ

Fig. 11(a), (b) reflects the size of periodic and chaotic pressure intervals corresponding to Fig. 10(a), (b) respectively. Fig. 11(a) shows that the periodic and the chaotic pressure intervals was interlaced with each other. When ξ was selected to be 0.6, 0.65 and 0.7, the chaotic pressure interval will be the maximum at $\xi = 0.7$ and the minimum at $\xi = 0.6$ during the 0-2000 N of brake pressure. Therefore, the large value of ξ will improve the characteristics of vibration of brake system. When α was selected to be 1, 2 and 3, the chaotic pressure interval will be the maximum

at $\alpha = 1$ and the minimum at $\alpha = 3$ during the same pressure range mentioned above, as shown in Fig. 11(b). Thus, the smaller value of α could also improve the characteristics of system vibration. Through the analysis, we can find that the chaotic pressure intervals could shrink by decreasing $\mu_k - \mu_s$ and retarding its rate of decay, therefore to improve the vibration characteristics of brake system.

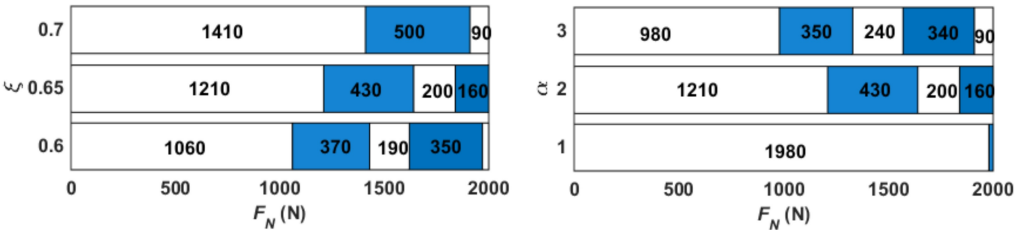

Fig. 11. The approximate periodic and chaotic pressure intervals under different α and ξ. (White – periodic pressure interval, blue – chaotic pressure interval)

6. Conclusions

1) According to Ref. [15], the torsional dynamic model which is coupled through a friction pair and under the condition of brake release on takeoff, we establish the mathematical model of four degrees of freedom torsional system under ideal braking conditions, then we studied the stick-slip motions of the system based on the selected friction model by numerical method. Our analysis reveals that the dynamic characteristics of the system could be converting from doubling periodic bifurcation to chaos by increasing the brake pressures.

2) The doubling periodic bifurcation is consists of two branches, the upper branch and lower branch. The bifurcation on the slip phase corresponds to the upper branch, while the fluctuations of relative velocities of stick phase corresponds to the lower branch. With the increase of brake pressures, the fluctuation of relative velocities becomes larger and larger that it can never be regarded as fluctuation in the stick phase, but the slip motion. In the test, the 'stick' and 'slip' appear to be irregular, then stick-slip motion gradually turns to chaos.

3) The Lyapunov exponent of the chaotic interval can be obtained by 'CLDYN' method, and verified by comparing it with the corresponding bifurcation diagram, where the maximum Lyapunov exponent can successfully distinguish the periodic motions from the chaotic intervals.

4) The effect of friction model parameter on bifurcation and chaos of the system has been studied to shrink the chaotic pressure interval by decreasing both the exponential decay factor α and increasing the ratio of the kinetic friction coefficient and the static friction coefficient ξ.

5) The future work will focus on any experimental researches on stick-slip vibrations to verify the discovery about the effects of brake pressures on bifurcation and chaos of brake systems, trying to find the influence of brake pressure both on periodic and chaotic interval, and thereafter providing theoretical and experimental support to reduce the chaotic interval at low braking speeds and to avoid any chaotic vibration of this type.

Acknowledgements

This research was supported by the National Science Foundation of China (No. 51375130 and No. 51050002).

References

[1] **Kinkaid N. M., O'Reilly O. M., Papadopoulos P.** Automotive disc brake squeal. Journal of Sound and Vibration, Vol. 267, 2003, p. 105-166.

[2] **Papinniemi Antti, Lai Joseph C. S., Zhao Jiye, Loader Lyndon** Brake squeal: a literature review. Applied Acoustics, Vol. 63, 2002, p. 391-400.

[3] **Wang Liang-mo** A review of a study on disc brake noise. International Journal of Plant Engineering and Management, Vol. 11, 2006, p. 242-246.

[4] **Guan Di-hua, Su Xin-dong** An overview on brake vibrations and noise. Engineering Mechanics, Vol. 21, Issue 4, 2004.

[5] **Mills H. R.** Brake Squeak. Technical Report 9000 B, Institution of Automobile Engineers, 1938.

[6] **Bowden F. P., Leben L.** The nature of sliding and the analysis of friction. Royal Society of London Proceedings Series a Mathematics Physics and Engineering Science, Vol. 169, 1939, p. 371-391.

[7] **Morgan F., Musjat M., Reed D. W.** Friction phenomena and the stick-slip process. Journal of Applied Physics, Vol. 12, Issue 10, 1941, p. 743-752.

[8] **Van De Velde F., De Baets P.** The relation between friction force and relative speed during the slip-phase of a stick-slip cycle. Wear, Vol. 219, 1998, p. 220-226.

[9] **Andreaus U., Casini P.** Dynamics of friction oscillators excited by a moving base and/or driving force. Journal of Sound and Vibration, Vol. 245, Issue 4, 2001, p. 685-699.

[10] **Li Yong, Feng Z. C.** Bifurcation and chaos in friction-induced vibration. Communications in Nonlinear Science and Numerical Simulation, Vol. 9, Issue 6, 2004, p. 633-647.

[11] **Canudas de Wit C., Olsson H., Astrom K. J., Lischinsky P.** A new model for control of systems with friction. IEEE Transactions on Automatic Control, 1995, p. 419-425.

[12] **Oestreich M., Hinrichs N., Popp K.** Bifurcation and stability analysis for a non-smooth friction oscillator. Archive of Applied Mechanics, Vol. 66, Issue 5, 1996, p. 301-314.

[13] **Vielsack Peter** Stick-slip instability of decelerative sliding. International Journal of Non-Linear Mechanics, Vol. 36, 2001, p. 237-247.

[14] **Shin K., Brennan M., Oh J., Harris C.** Analysis of disc brake noise using a two-degree-of freedom model. Journal of Sound and Vibration, Vol. 254, Issue 5, 2002, p. 837-848.

[15] **Shin Kihong, Oh Jae-Eung, Brennan Michael J.** Nonlinear analysis of friction induced vibrations of a two-degree-of-freedom. JSME International Journal, Vol. 45, Issue 2, 2002, p. 426-432.

[16] **Paliwal Manish, Mahajan Ajay, Don Jarlen, Chu Tsuchin, Filip Peter** Noise and vibration analysis of a disc–brake system using a stick-slip friction model involving coupling stiffness. Journal of Sound and Vibration, Vol. 282, 2005, p. 1273-1284.

[17] **Yang F. H., Zhang W., Wang J.** Sliding bifurcations and chaos induced by dry friction in a braking system. Chaos, Solitons and Fractals, Vol. 40, Issue 3, 2009, p. 1060-1075.

[18] **Li Bo, Ding Qian** Numerical study on the self-excited vibration of disc brake system. Science and Technology Review, Vol. 25, Issue 23, 2008, p. 28-32.

[19] **Crowther A. R., Singh R.** Analytical investigation of stick-slip motions in coupled brake-driveline system. Nonlinear Dynamics, Vol. 50, 2007, p. 463-481.

[20] **Crowther A. R., Singh R.** Identification and quantification of stick-slip induced brake groan events using experimental and analytical investigations. Noise Control Engineering Journal, Vol. 56, Issue 4, 2008.

[21] **Zhang Jin, Zhang Nong, Crowther Ashliy R.** Analytical study of brake groan through a coupled 2DOF brake model. Industrial and Applied Mathematics Japan, Vol. 28, 2011, p. 205-222.

[22] **Berger E. J.** Friction modeling for dynamic system simulation. Applied Mechanics Reviews, Vol. 55, Issue 6, 2002, p. 535-577.

[23] **Duan Chengwu, Singh Rajendra** Stick-slip behavior of torque converter clutch. SAE Paper, 2005, p. 2005-01-2456.

[24] **Jang H., Lee J. S., Fash J. W.** Compositional effects of the brake friction material on creep groan phenomena. Wear, Vol. 251, 2001, p. 1477-1483.

[25] **Soriano Diogo C., Fazanaro Filipe I., Suyama Ricardo, de Oliveira José Raimundo, Attux Romis, Madrid Marconi K.** A method for Lyapunov spectrum estimation using cloned dynamics and its application to the discontinuously-excited FitzHugh-Nagumo model. Nonlinear Dynamics, Vol. 67, 2012, p. 413-424.

[26] **Shan Huanle., Mo Jiliang, Chen Guangxiong, Shao Tianmin, Zhou Zhongrong** Effects of grooved surface texture on friction noise. Chinese Journal of Mechanical Engineering, Vol. 23, Issue 18, 2012, p. 2233-2237.

[27] **Menezes Pradeep L., Kishore, Kailas Satish V.** Effect of surface roughness parameters and surface texture on friction and transfer layer formation in tin–steel tribo-system. Journal of Materials Processing Technology, Vol. 208, 2008, p. 372-382.

[28] **Menezes Pradeep L., Kishore, Kailas Satish V.** Influence of surface texture and roughness parameters on friction and transfer layer formation during sliding of aluminium pin on steel plate. Wear, Vol. 267, 2009, p. 1534-1549.

Daogao Wei received Ph.D. degree in School of Automotive and Traffic Engineering from Jiangsu University, Jiangsu, China, in 2003. Now he is an Associate Professor at School of Mechanical and Automotive Engineering, Hefei University of Technology. His current research interests include vehicle system dynamics and nonlinear dynamics.

Weiwei Zhu is a Master of School of Mechanical and Automotive Engineering, Hefei University of Technology – Hefei, China. His current research interests include structure vibration and noise analysis and nonlinear dynamics.

Bo Wang is a Master of School of Mechanical and Automotive Engineering, Hefei University of Technology – Hefei, China. His current research interests include brake vibration and noise analysis and nonlinear dynamics.

Qian Ma received her M.S. degree in School of Mechanical and Automotive Engineering from Hefei University of Technology, Hefei, China, in 2013. Now she works at XCMG. Her research interests include vehicle system dynamics, noise and vibration control, and the load spectrum test of the transmission system.

Zuheng Kang is a Master of Science Candidate of University of Missouri – Columbia, USA. Now his research preference is control, dynamics and mathematical modelling.